High-rate hydrogenotrophic denitrification in a pressurized reactor

Razi Epsztein *, Michael Beliavski, Sheldon Tarre, Michal Green

Faculty of Civil and Environmental Engineering, Technion – Israel Institute of Technology, Haifa 32000, Israel

HIGHLIGHTS

- A novel pressurized H_2-based reactor for denitrification is presented.
- The common misconception of N_2 accumulation in closed headspace is eliminated.
- At steady-state, N_2 pressure remains constant and no gas purging is required.
- The reactor presents high rates of approximately 5 g NO_3^--N/($L_{reactor}$ d).
- Hydrogen utilization efficiencies of up to 96.9% are achieved.

ARTICLE INFO

ABSTRACT

Most conventional hydrogenotrophic denitrification reactors based on packed- or fluidized-bed present a similar H_2 delivery scheme of continuous gas purging to the atmosphere in order to improve H_2 transfer rates and enable discharge of N_2 gas produced during denitrification. This operation results in a significant release of H_2 gas to atmosphere with its related economic and safety concerns. The current research proposes a novel pressurized high-rate hydrogenotrophic reactor for denitrification without gas purging. The investigation performed refutes a prevalent notion that N_2 gas accumulates in the headspace of a closed reactor during denitrification. Instead, this research shows that during continuous operation a gas–liquid equilibrium is established in the reactor according to Henry's law and excess N_2 gas is carried out by the effluent in dissolved form. Therefore, no gas purging is required and H_2 loss is limited only to the dissolved H_2 in the effluent. As a consequence, a simple low-cost and high-rate reactor with closed headspace can be designed for denitrification. The proposed reactor is operated as a trickling filter where water is recirculated over biofilm carriers with high surface area.

The feasibility of the proposed reactor was shown for two effluent concentrations of 10 and 1 mg NO_3^--N/L. Average denitrification rates of 2.1 ± 0.2 and 1.06 ± 0.06 g NO_3^--N/($L_{reactor}$ d) with H_2 utilization efficiencies of 92.8% and 96.9% were measured for the two effluent concentrations, respectively. Higher denitrification rates of up to 5 g NO_3^--N/($L_{reactor}$ d) were observed at higher recirculation flow rates and higher partial pressures of H_2.

1. Introduction

Biological denitrification of nitrate-contaminated groundwater has been widely investigated with both heterotrophic [1,2] and autotrophic [3] cultures. The more common process of heterotrophic denitrification, where nitrate is reduced by various organic compounds, is characterized by high efficiency and high denitrification rates [4]. However, the main drawbacks of biological denitrification of drinking water using heterotrophic cultures are the potential risk of microbial contamination of the treated water, the remaining of organic metabolites and microbial products,

excess waste biomass and reactor clogging, formation of disinfection by-products (DBP) and costly post-treatment [5].

Autotrophic denitrification using reduced inorganic compounds as electron donor and CO_2 as carbon source, overcomes most of the above disadvantages. Reactor clogging, waste sludge production and post-treatment costs are reduced due to significantly less biomass growth. Autotrophic denitrification using H_2 gas, also named hydrogenotrophic denitrification, is an excellent choice because of its clean nature and low biomass yield, as well as the fact that H_2 does not persist in the treated water. Moreover, H_2 is less expensive than other electron donors. However, the main drawbacks limiting the use of hydrogenotrophic denitrification are safety concerns, poor H_2 utilization and low denitrification rates due to low solubility of H_2 with the resulting low transfer rate [6].

A summary of the prior research on hydrogenotrophic denitrification is shown in Table 1. Most of the investigated packed/fluidized-bed hydrogenotrophic systems lack efficient and safe delivery of H_2 and present a similar H_2 delivery scheme of gas sparging in either a separate H_2 saturation tank [7] or a main reactor tank [8]. Membrane biofilm reactors (MBfRs) and bio electrochemical reactors (BERs) were both designed to enable more efficient, safer and high-rate H_2 delivery to biofilm. The MBfR technology has already been proven successfully on both pilot scale and even full scale. However, results from MBfRs reveal low denitrification rates due to the limited surface area available for biofilm growth [9–12]. Moreover, MBfRs are costly due to the high cost of membrane replacement and cleaning because of fouling [13]. BERs also suffer from limited surface area available for biofilm growth and low denitrification rates [14–16]. Additionally, a gradual scale formation on the surface of the cathode suppresses H_2 production [17].

Table 1 shows that H_2-based reactors reach denitrification rates above 0.5 g NO_3^--N/($L_{reactor}$ d) only when a wasteful H_2 delivery scheme of bubbling was applied (e.g. packed- and fluidized-bed systems with bubbling). Safe and economic systems (e.g. BERs and MBfRs) could not reach high rates, mainly due to a limited surface area for biofilm growth. In other words, a process combines high rates with safe and economic operation is yet to be achieved.

To the best of our knowledge, there are no reports of hydrogenotrophic systems based on pressurized reactors without gas purging. The main reason is assumed to be a possible misconception claiming that during denitrification in a closed-headspace reactor, N_2 gas build-up occurs in the reactor's headspace and requires intermittent or continuous gas purging.

The current work presents a novel pressurized high-rate hydrogenotrophic reactor without gas purging, as shown in Fig. 1. The reactor is described in detail in Section 2. Briefly, the operation of the reactor maintains a gas–liquid equilibrium without pressure build-up of N_2 gas and without any H_2 gas loss from the gas phase. The reactor is operated under an unsaturated-flow regime as a trickling filter where water is recirculated over the biofilm carriers. Plastic carriers with large surface area are used and together with high mass transfer of H_2 gas, high denitrification rates are achieved [18]. The main objective of the following research is to prove the suggested concept that during continuous operation N_2 gas reaches a gas–liquid equilibrium without further accumulation in the closed headspace of denitrifying reactor. The second goal is to show how the new concept facilitates the design of an applicable reactor capable of operating at high denitrification rates.

Table 1
Denitrification rates of various systems and H_2 delivery schemes.

Reactor type/H_2 delivery scheme	Denitrification rate [g NO_3^--N/($L_{reactor}$ d)]	References
BER/as described above	0.06	[14]
	0.393	[23]
MBfR/as described above	0.182	[11]
	0.2–0.5	[9]
Packed-bed/H_2 saturation in separate tank with electrolysis	0.25	[17]
Packed-bed/H_2 saturation in separate tank with gas-permeable membrane	0.471	[24]
Packed-bed/direct bubbling	2.5[a]	[8]
Packed-bed/unsaturated flow (trickling filter)	0.036	[25]
Fluidized-bed/bubbling in separate saturation tank	0.552	[7]
Fluidized-bed/direct bubbling	0.6–0.7	[26]
Suspended growth with MBR/saturation in separate tank under pressure	0.11	[27]

[a] The denitrification rate is 6.2 g NO_3^--N/(L d) based on media porosity.
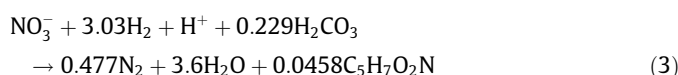
2. Description of the proposed reactor

A schematic diagram of the proposed reactor is illustrated in Fig. 1. The reactor is operated under an unsaturated flow regime where water is recirculated and trickled over biofilm carriers. The reactor is continuously fed with nitrate-contaminated groundwater. When enough liquid collects at the reactor's bottom and reaches a level switch, a drain valve is opened and treated water is released (i.e. pulsed discharge). The reactor's gas phase is closed to the atmosphere and pressurized by the supplied H_2 and the N_2 formed during denitrification. An additional source of N_2 gas is atmospheric N_2 dissolved in the influent water and carried into the reactor, where it can desorb.

The key feature of the proposed reactor is its ability to reach a gas–liquid equilibrium and maintain constant partial pressures of both H_2 and N_2 gases without further accumulation of N_2 gas over time. This ability is achieved only under continuous operation where effluent water carries excess of N_2 gas out of the reactor. At the beginning of the process, N_2 in the liquid phase includes only atmospheric N_2 (i.e. dissolved N_2 originating from air), thus partial pressure of N_2 in the gas phase is approximately 0.8 bars (as in normal air mixture). The reactor is then pressurized by H_2 gas to the desired total pressure. Over time N_2 gas is produced by hydrogenotrophic denitrification and exchanges H_2 gas in the gas phase, so the partial pressure of N_2 gas increases and the partial pressure of H_2 gas decreases. At some point, the partial pressure of N_2 gas reaches a level correlating with the terminal N_2 concentration in the liquid phase according to Henry's law, a gas–liquid equilibrium is achieved and the partial pressures of both N_2 and H_2 gases in the gas phase remain constant. Therefore, the final partial pressure of N_2 gas depends directly on N_2 concentration in the influent (i.e. the atmospheric N_2) and the concentration of NO_3^--N removed and converted to N_2 gas.

In order to introduce H_2 gas and enable denitrification, the total pressure applied (i.e. pressure of N_2 and H_2) must be higher than the partial pressure of N_2 at gas–liquid equilibrium. Fig. 2 presents the partial pressure of N_2 in the reactor at gas–liquid equilibrium and 25 °C, as a function of NO_3^--N concentration removed according to Eq. (1). In Eq. (1), P_{N_2} is the partial pressure of N_2 in the reactor, $P_{N_2,atm}$ is the N_2 pressure resulting from atmospheric N_2 (i.e. ~0.8 bars) and $P_{N_2,denitrification}$ is the N_2 pressure resulting from N_2 gas produced during denitrification and calculated by Eq. (2). In Eq. (2), $C_{N_2,denitrification}$ is the concentration of NO_3^--N converted to N_2, and H_{N_2} is Henry's constant (17 mg N_2/(L bar) at 25 °C). The calculations for $C_{N_2,denitrification}$ are based on previous suggested stoichiometry of hydrogenotrophic denitrification according to Eq. (3). For simplification and due to low biomass yield, it was assumed that all NO_3^--N consumed was converted to N_2 [6].

$$P_{N_2} = P_{N_2,atm} + P_{N_2,denitrification} \qquad (1)$$

$$P_{N_2,denitrification} = C_{N_2,denitrification}/H_{N_2} \qquad (2)$$

$$NO_3^- + 3.03H_2 + H^+ + 0.229H_2CO_3$$
$$\rightarrow 0.477N_2 + 3.6H_2O + 0.0458C_5H_7O_2N \qquad (3)$$

For lower concentrations of NO_3^--N removed, less N_2 is produced by denitrification per volume of water so the resulting partial pressure of N_2 is lower. Alternatively, for a specific total pressure of N_2 and H_2, a lower NO_3^--N concentration removal will result in a lower partial pressure of N_2 with a corresponding higher partial pressure of H_2. For typical conditions of an inlet NO_3^--N concentration of 25 mg/L and a projected reactor effluent at drinking water regulations of 10 mg NO_3^--N/L (15 mg/L NO_3^--N removed), the partial pressure of N_2 in the reactor at gas–liquid equilibrium is calculated to be 1.7 bars (see Fig. 2). Therefore, the minimal total
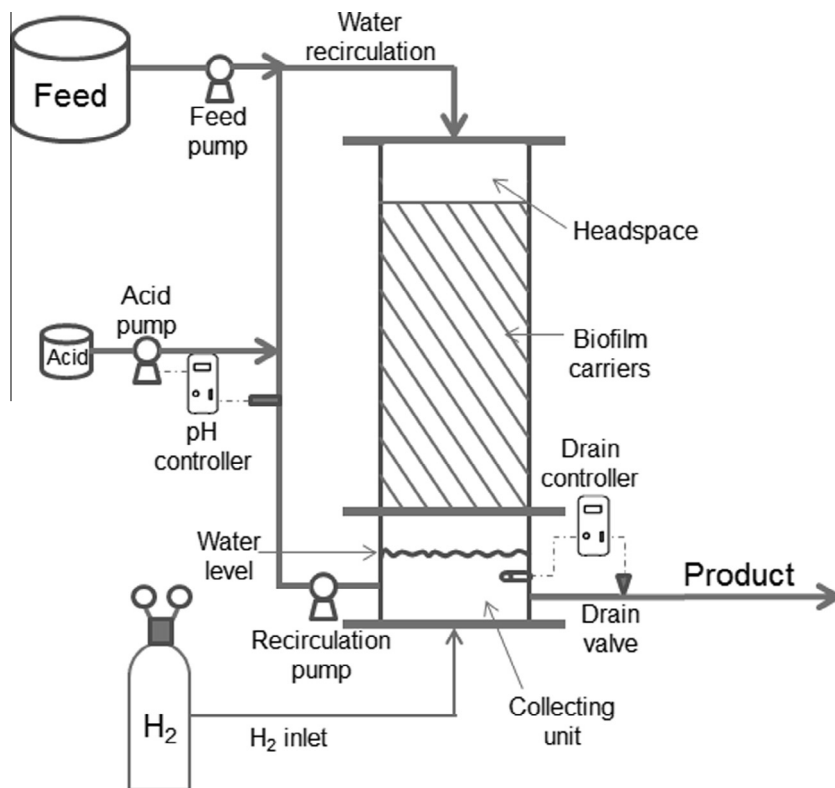
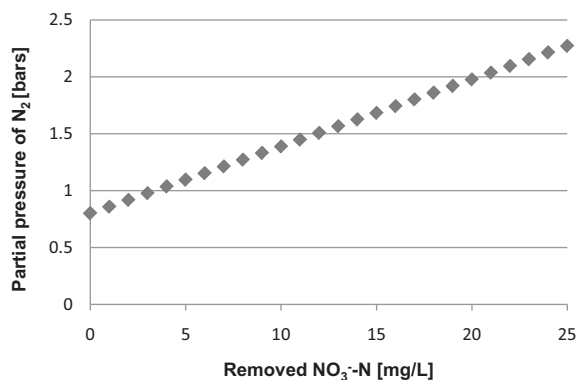Fig. 1. Schematic diagram of the proposed reactor.

Fig. 2. Partial pressure of N_2 in the reactor at gas–liquid equilibrium and 25 °C, as a function of NO_3^--N concentration removed.

pressure applied to the pressurized reactor must be above this value. For example, applying a total pressure of 2 bars leaves room for 0.3 bars of H_2.

In terms of safety and economics, this property of maintaining constant pressure of N_2 eliminates the need for reactor gas discharge with the accompanying H_2 loss to atmosphere as occurs in conventional systems described in the former section. Moreover, at gas–liquid equilibrium the pressurized reactor contains an inert N_2–H_2 gas mixture without O_2 gas, so that the formation of an explosive atmosphere within the reactor is prevented. Finally, working under low partial pressure of H_2 minimizes risks in case of failures and reduces H_2 loss to the liquid phase, i.e. residual H_2 that was not consumed.

In addition to the above mentioned advantages of safety and economics, the proposed reactor allows for high denitrification rates in comparison to existing hydrogenotrophic systems. The reactor contains carriers with high surface area that allows for better dispersal and thin biofilm development. This leads to a more effective biomass at relatively low H_2 partial pressures with a corresponding low dissolved H_2 concentration. The large gas–liquid contact area provided by the carriers together with the high diffusion coefficient of H_2 in the gas phase of the reactor ensures that a high mass transfer rate of H_2 is achieved.

3. Materials and methods

3.1. Experimental setup

The reactor system used for all tests is shown in Fig. 1. It comprised of a clear PVC cylindrical reactor 71 cm in height and 10.5 cm in diameter divided into two unequal parts. The top part of the reactor (height 51 cm) contained plastic biofilm carriers (total surface area of 900 m^2/m^3, Aqwise) and was separated by a metal screen from the bottom part (height 20 cm) of the reactor where recirculating water collected. The reactor was connected to a gas supply (H_2 cylinder with pressure regulator), feed pump (Diaphragm pump model 7090-42, Cole-Palmer), recirculation pump (FL-2403, ProPumps) and pH controlling unit (standard pH electrode, pH controller – pH190, Alpha; hydrochloric acid tank and acid pump – gamma/L, ProMinent).

For reactor start-up, a 2 L solution consisting of tap water enriched with nitrate, bicarbonate (added as 2 g of $NaHCO_3$) and phosphate with 0.5 L bacteria originating from a former hydrogenotrophic reactor was prepared and recirculated through the reactor under a constant H_2 pressure of 2 bars by purging. The feed solution for all experiments was tap water mixed with concentrated stock solutions of $NaNO_3$ and KH_2PO_4 (influent concentration of 1 mg P/L). Except for the experiment of checking the influence of recirculation flow rate on denitrification rates, recirculation flow rate was 2500 mL/min for all trials. Water

temperature was maintained constant at 25.5 ± 1 °C. pH was kept at 7.1 by dosing hydrochloric acid. The relatively low pH was aimed to prevent an extreme pH increase within the biofilm, which leads to NO_2^--N accumulation [19,20]. Influent and effluent water were collected for further analyses.

3.2. Analyses

Nitrate concentration was determined using a Metrohm 761 ion chromatograph (IC) equipped with a 150 mm Metrosep A Supp 5 column with column guard and suppressor using a CO_3^{2-}/HCO_3^- eluent. Nitrite-N concentration and alkalinity were measured according to Standard Methods (Method 4500 and Method 2320, respectively). H_2 concentration in gas phase was measured by gas chromatography (TCD detector; column: HP-PLOT-Q 30 m; 0.53 mm, 40μ, Agilent 7890A). Samples for the gas phase analysis by gas chromatography were taken by direct injection of fresh gas mixture from the reactor headspace into a 20 mL sealed serum bottle. The bottle was first flushed with the same gas mixture from the reactor headspace for 1 min with gas flow rate of 250 mL/min to ensure exchange of the entire gas volume in the bottle. The dissolved H_2 concentration in liquid phase was measured by headspace analysis of effluent samples immediately sealed within a serum bottle using the same gas chromatograph.

3.3. Test protocols

3.3.1. Effect of total pressure and NO_3^--N concentration on denitrification rates

Denitrification rates of the proposed reactor were initially tested for various combinations of total pressure and effluent NO_3^--N concentration with constant recirculation flow rate of 2500 mL/min. For each total pressure tested, the system was first operated to steady state with high effluent NO_3^--N concentration (>15 mg/L). The time required to reach a steady state ranged between 1 and 2 days. The total pressures applied were 1.5, 2, 2.5 and 3 bars. For the current research purposes, steady state was defined as an operational state presenting constant denitrification rate during extended operation. After reaching steady state, the effluent NO_3^--N concentration was decreased gradually by adjusting the influent NO_3^--N concentration and the denitrification rate was calculated for each combination of total pressure and effluent NO_3^--N concentration (see Section 4.1). Due to relatively short retention time (see Section 4.2), the measurements for each total pressure could be performed during a short period of less than 3 h. In such a short time, it was assumed that gas phase composition remained constant. The inlet NO_3^--N concentration was operated in the range of 3–35 mg/L (added as NaNO₃) and the influent flow rate was kept constant on 450 mL/min. Reactor cleaning by flushing with water was carried out every few days to remove excess biomass growth. The frequency of cleaning depended on the denitrification rate achieved for different operational parameters.

3.3.2. Effect of recirculation flow rate on denitrification rates

In a second set of experiments, the influence of recirculation flow rate on denitrification rates was tested. In this case, the H_2 pressure applied was 3 bars and the effluent NO_3^--N was kept constant on 5 mg/L by adjusting the inlet NO_3^--N concentration in the range of 15–40 mg NO_3^--N/L (added as NaNO₃). In this specific experiment (as opposed to the standard operation of the proposed reactor), the H_2 pressure was kept constant by continuous flushing of the reactor headspace with H_2 gas. The reactor was first operated at the highest recirculation flow rate of 8000 mL/min. After reaching steady state, the recirculation flow rate was decreased

gradually and denitrification rates and effluent dissolved H_2 concentrations were measured for each recirculation flow rate applied.

Liquid retention times for different recirculation flow rates were measured by the following procedure: (1) reactor was completely drained and then was filled with the carriers (covered with biomass); (2) an influent flow rate of 450 mL/min was applied without recirculation and the time till the first reactor drain was measured. This measurement gave the liquid retention time without recirculation; (3) recirculation flow rate was then increased gradually and the lag between two drains was measured. This lag was the addition to the liquid retention time due to the increase in recirculation flow rate.

3.3.3. Proof of concept – reaching a gas–liquid equilibrium

After investigating the effect of total pressure, NO_3^--N concentration and recirculation flow rate on denitrification rates, the concept of reaching a steady state with constant partial pressures of both H_2 and N_2 gases was further tested for two operational modes: (i) operation with high effluent NO_3^--N concentration of 10 mg/L, and (ii) operation with low effluent NO_3^--N concentration of 1 mg/L. The inlet NO_3^--N concentration was 25 mg/L for both operations. The influent flow rates applied for operations (i) and (ii) were 430 and 130 mL/min, respectively. For each operation, the total pressure applied was determined by summing the theoretical N_2 partial pressure developed (Fig. 2) with the H_2 partial pressure needed (Fig. 3) as will be described in Section 4.2. The recirculation flow rate was 2500 mL/min for both operations.

Each operation started with pressurizing the reactor with H_2 gas to the desired total pressure above the atmospheric pressure (e.g. for total absolute pressure of 3 bars, 2 bars of H_2 gas were added above the atmospheric pressure). The total pressure was maintained constant throughout the experiment by keeping the H_2 cylinder connected to the reactor through a pressure regulator. The concentration of H_2 gas in the reactor headspace was measured over time and converted to partial pressure. Assuming H_2 and N_2 are the only gases in the reactor (after initial oxygen depletion), the partial pressure of N_2 gas could also be calculated by subtracting the partial pressure of H_2 from the total pressure. At the beginning of the process, this subtraction gives the partial pressures of both N_2 and O_2.

All denitrification rates in this paper were calculated based on the empty reactor volume excluding the volume of the collecting unit.

4. Results and discussion

4.1. Effect of total pressure and NO_3^--N concentration on denitrification rates

Fig. 3 presents the denitrification rates calculated after reaching steady state, as a function of effluent NO_3^--N concentration for 4 different total pressures as described in Section 3.3.1.

A similar trend was observed for all total pressures tested. Nitrate was limiting at low NO_3^--N concentrations (e.g. NO_3^--N < ∼5 mg/L for the experiment with total pressure of 2.5 bars). At higher NO_3^--N concentrations (e.g. NO_3^--N > ∼5 mg/L for the experiment with total pressure of 2.5 bars), total pressure was found to govern denitrification rate. This is due to the different H_2 partial pressures achieved (with the corresponding different dissolved H_2 concentration) for each total pressure applied. The H_2 partial pressure could be estimated using the theory proposed in Section 2 and summarized in Fig. 2. For example, for the lowest total pressure of 1.5 bars, a denitrification rate of 0.7 g N/(L_reactor d) was achieved at steady state. The removal of NO_3^--N in this case was approximately 5 mg/L that correlates to a N_2 partial pressure buildup of 1.1 bars according to Fig. 2. Therefore the H_2 partial
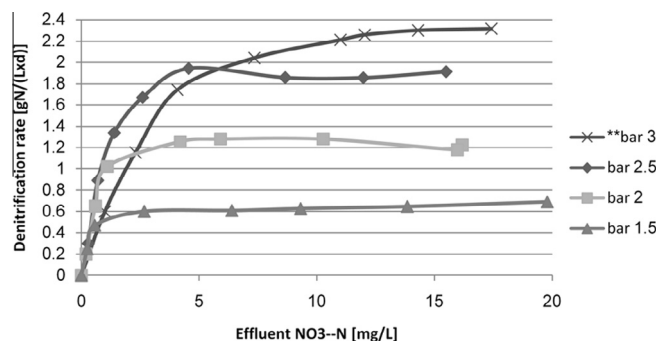
Fig. 3. Denitrification rate as a function of effluent NO_3^--N concentration for 4 different total pressures of 1.5, 2, 2.5 and 3 bars. [**]For the experiment with 3 bars, the reactor was maintained at pH 6.8 (see explanation in text).

pressure calculated was the difference between the total pressure and the N_2 partial pressure, i.e. 0.4 bars. The H_2 partial pressures calculated for the trials with total pressures of 2, 2.5 and 3 bars were 0.7, 1 and 1.3 bars, respectively. In general, with higher H_2 partial pressure, higher denitrification rates could be achieved and the NO_3^--N concentration in which the transition to H_2 limitation occurred was also higher. Fig. 3 shows the potential of the proposed reactor to operate at high denitrification rates as compared to previously reported hydrogenotrophic systems with a maximal rate of more than 2.1 g NO_3^--N/($L_{reactor}$ d) for operation with H_2 partial pressure of 1.3 bars and 10 mg/L of effluent NO_3^--N.

Penetration to deeper biofilm layers at higher H_2 partial pressure results in higher pH rise in the biofilm. Previous reports link high pH to NO_2^--N accumulation [19,20]. At bulk pH of 7.1, NO_2^--N accumulation in the effluent was negligible for the experiments with 0.4, 0.7 and 1 bars for all effluent NO_3^--N concentrations. However, when a H_2 partial pressure of 1.3 bars was tested (i.e. total pressure of 3 bars) together with effluent NO_3^--N concentrations of 7 mg/L and higher, an effluent NO_2^--N concentration of approximately 2 mg/L was measured, probably due to the extreme pH rise within the biofilm. Therefore, the bulk pH in the reactor was lowered to 6.8 after which effluent NO_2^--N concentrations were below detection limits. The operation under lower bulk pH may lead to a slight inhibition of bacterial activity in the outer layers of the biofilm, which can also explain the moderate shift of the curve to the right in the case of operation under H_2 partial pressure of 1.3 bars.

4.2. Effect of recirculation flow rate on denitrification rates

A second set of experiments was performed in order to determine the effect of recirculation flow rate (Q_R) on denitrification
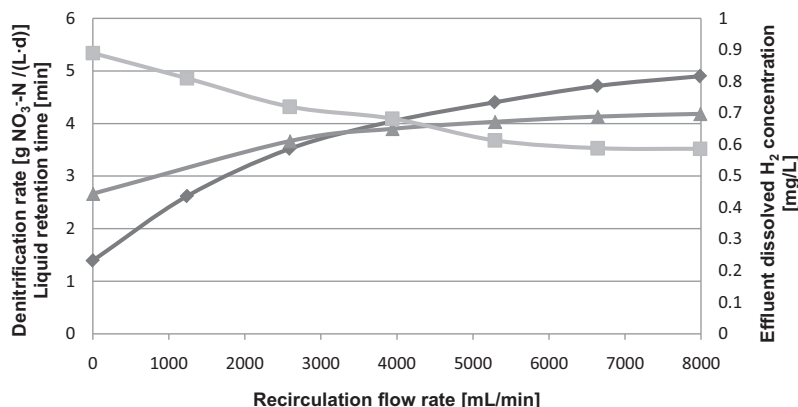
rates. The experiment was conducted at higher H_2 pressure of 3 bars to ensure that hydrogen would not be limiting and thus to achieve higher denitrification rates. Effluent NO_3^--N was kept constant on 5 mg/L by controlling the inlet NO_3^--N concentration. In addition to Q_R, the influent flow rate (Q) was 450 mL/min. The denitrification rates, liquid retention time and effluent dissolved H_2 concentration achieved as a function of the recirculation flow rate are shown in Fig. 4.

Denitrification rates increased significantly with higher recirculation flow rates. These increased rates can be partially explained by the moderate increase in liquid retention time. The main reason for the improved denitrification rate is probably the increase in media wetting which results in higher surface area of active biofilm exposed to both NO_3^--N and H_2. The lowest denitrification rate was observed for operation without any recirculation (i.e. $Q_R = 0$). In this case, wetting of media was achieved only by the influent flow (i.e. $Q = 450$ mL/min). At $Q_R \approx 8000$ mL/min, media wetting appears to approach a maximal level accompanied by a denitrification rate of close to 5 g NO_3^--N/($L_{reactor}$ d). This rate is much higher than any rate reported in previous investigations (see Table 1).

The gradual decrease in effluent dissolved H_2 at higher recirculation flow rates is a result of the higher H_2 consumption rate in the biofilm. This supports the assumption that higher denitrification rates were achieved due to better media wetting rather than better gas (H_2)-liquid transfer and deeper penetration of H_2 in the biofilm. Further increase of Q_R was not possible due to technical issues. Water recirculation is also known to be a crucial feature in the process design of trickling filters for BOD and ammonia degradation. When the hydraulic load is too low, recirculation of water is applied to enhance the reactor efficiency by maximizing media wetting and minimizing channeling and poor horizontal mixing [21,22].

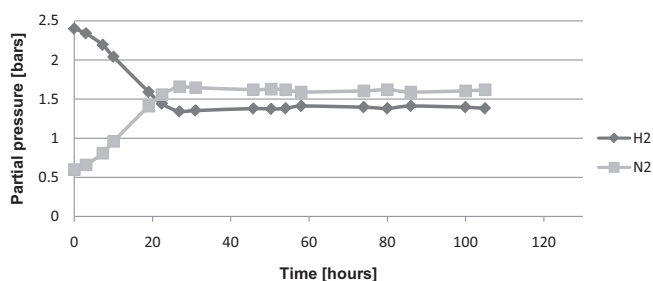### 4.3. Proof of concept – reaching a gas–liquid equilibrium

After determining the effect of total pressure, NO_3^--N concentration and recirculation flow rate on denitrification rates in the hydrogenotrophic reactor, two operational modes with different effluent NO_3^--N concentration and total pressure were chosen (Table 2) for proving the concept of reaching a gas-liquid equilibrium in a pressurized reactor without gas purging. The same recirculation flow rate of 2500 mL/min was applied as in Section 4.1. In Table 2, the total pressure in the reactor needed to achieve a maximal denitrification rate for a specific effluent NO_3^--N concentration was determined by combining the information presented in Fig. 2 (N_2 partial pressure) and Fig. 3 (H_2 partial pressure).

Operation (i) simulates the common treatment process aimed to meet the worldwide regulations for NO_3^--N in drinking water.

Fig. 4. Denitrification rate (diamonds), liquid retention time (triangles) and effluent dissolved H_2 concentration (squares) as a function of recirculation flow rate at constant effluent NO_3^--N concentration of 5 mg/L and H_2 pressure of 3 bars.

Table 2
Detailed description of operational modes tested for proving the concept of reaching a gas–liquid equilibrium.

Operation	Inlet NO_3^--N [mg/L]	Effluent NO_3^--N [mg/L]	N_2 pressure developed at 25 °C (Fig. 2) [bars]	H_2 pressure needed for maximal rate (Fig. 3) [bars]	Total pressure needed [bars]
(i)	25	10	1.7	1.3	3
(ii)	25	0–1	2.3	0.7	3

Fig. 5. Partial pressure of H_2 (diamonds) and N_2 (squares) gases in the reactor headspace as a function of time for operation (i) (effluent NO_3^--N = 10 mg/L).
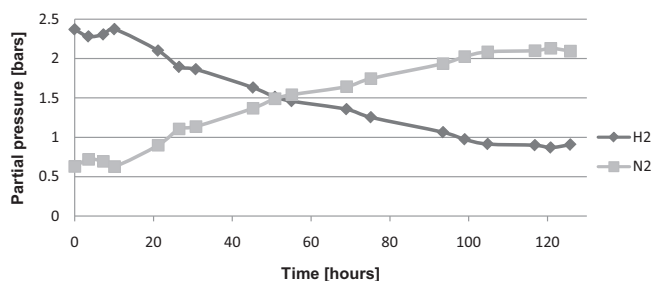
Fig. 6. Partial pressure of H_2 (diamonds) and N_2 (squares) gases in the reactor headspace as a function of time for operation (ii) (effluent NO_3^--N = 1 mg/L).

A common alternative practice is to treat a portion of NO_3^--N containing groundwater to very low concentrations (e.g. ~1 mg/L) and to mix the low concentration product water with untreated groundwater to meet the drinking water standard. This type of operation, sometimes called split treatment process, is represented by operation (ii). According to Table 2, for both operational modes at $t = 0$ the reactor was pressurized to 3 bars by introducing 2 bars of H_2 gas above atmospheric pressure, and the H_2 concentration in the reactor headspace was measured over time. Figs. 5 and 6 present the partial pressures of H_2 and N_2 gases in the reactor headspace as a function of time for operations (i) and (ii), respectively.

In general, a similar trend was observed for both operations. A constant increase in N_2 partial pressure (accompanied by constant decrease in H_2 partial pressure) occurred till a gas–liquid equilibrium was achieved and the partial pressure of both gases remained constant as hypothesized. With higher denitrification rate, operation (i) presented faster increase in N_2 partial pressure than operation (ii) before equilibrium was reached.

The average denitrification rates calculated for operations (i) and (ii) were 2.1 ± 0.2 and 1.06 ± 0.06 g NO_3^--N/($L_{reactor}$ d), respectively. The final partial pressures of N_2 achieved for operations (i) and (ii) were 1.6 and 2.1 bars, respectively. This small deviation from theoretical calculations for steady-state N_2 pressures (Table 2) can be attributed to the fact that the reactor is not a true completely mixed system. This results in higher NO_3^--N concentration at the top of the reactor (i.e. where less NO_3^--N is removed) with the corresponding lower partial pressure of N_2 produced according to the theory presented in Section 2. Alternatively, the deviation

mentioned may be explained by the density differences of H_2 and N_2 gases. The concentration of H_2, the lighter gas, at steady state was a bit higher than expected at the top of the reactor where the gas was sampled. This phenomenon of higher than expected H_2 concentration was observed also at the beginning of the process. The delay in the increase of the partial pressure of N_2 gas at the beginning of operation (ii) ($0 < t < 10$ h) is probably due to O_2 utilization combined with a lower denitrification rate.

At gas–liquid equilibrium (23 and 105 h for operations (i) and (ii), respectively), the residual H_2 concentrations in liquid phase (e.g. effluent H_2 that was not consumed) were 0.5 and 0.34 mg/L for operations (i) and (ii), respectively. According to Eq. (3), these dissolved H_2 concentrations correlate with H_2 gas utilization efficiencies of 92.8% and 96.9% for operations (i) and (ii), respectively. Further enhancement of utilization efficiency of H_2 is possible by passing the effluent through an additional downstream denitrifying reactor open to the atmosphere, so the residual H_2 can be further utilized. The average NO_3^--N concentrations measured throughout the experiments were 10.1 ± 1.2 and 1.3 ± 0.6 mg/L for operations (i) and (ii), respectively. Nitrite concentrations were always below detected levels for both operations.

5. Conclusions

A novel unsaturated-flow pressurized hydrogenotrophic reactor for denitrification without gas purging was successfully tested. The possible misconception regarding N_2 gas accumulation in a closed-headspace reactor was refuted by showing that in a continuous operation H_2 and N_2 in the gas phase reach a constant steady state concentration. This approach allows for safe and economic reactor operation in terms of H_2 gas utilization since no purging is required. Denitrification rates of one order of magnitude higher than most previously reported denitrification rates were achieved using a trickling filter with recirculation. Nitrate concentration and H_2 partial pressure were found to limit denitrification rates by partial penetration to biofilm. Higher recirculation flow rate could improve significantly denitrification rates up to 5 g NO_3^--N/($L_{reactor}$ d) by enhancing media wetting. The high surface area of the filter media available for bacterial growth and gas transfer allowed for working under low partial pressures of H_2 with utilization efficiencies of more than 92%.

References

[1] A. Mohseni-Bandpi, D.J. Elliott, M.A. Zazouli, Biological nitrate removal processes from drinking water supply – a review, J. Environ. Health Sci. Eng. 11 (2013) 35. <http://www.ijehse.com/content/11/1/35>.
[2] G. Liu, H. Zhang, W. Li, X. Zhang, Advances of external carbon source in denitrification, Adv. Mater. Res. 518–523 (2012) 2319–2323, http://dx.doi.org/10.4028/www.scientific.net/AMR.518-523.2319.
[3] I. Zhu, T. Getting, A review of nitrate reduction using inorganic materials, Environ. Technol. Rev. 1 (2012) 46–58, http://dx.doi.org/10.1080/09593330.2012.706646.

[4] V. Matějů, S. Čižinská, J. Krejčí, T. Janoch, Biological water denitrification – a review, Enzyme Microb. Technol. 14 (1992) 170–183, http://dx.doi.org/10.1016/0141-0229(92)90062-S.

[5] D. Cliford, X. Liu, Ion exchange for nitrate removal, Res. Technol. (1993) 135–143.

[6] K.A. Karanasios, I.A. Vasiliadou, S. Pavlou, D.V. Vayenas, Hydrogenotrophic denitrification of potable water: a review, J. Hazard. Mater. 180 (2010) 20–37, http://dx.doi.org/10.1016/j.jhazmat.2010.04.090.

[7] M. Kurt, I.J. Dunn, J.R. Bourne, Biological denitrification of drinking water using autotrophic organisms with H(2) in a fluidized-bed biofilm reactor, Biotechnol. Bioeng. 29 (1987) 493–501.

[8] I.A. Vasiliadou, K.A. Karanasios, S. Pavlou, D.V. Vayenas, Experimental and modelling study of drinking water hydrogenotrophic denitrification in packed-bed reactors, J. Hazard. Mater. 165 (2009) 812–824, http://dx.doi.org/10.1016/j.jhazmat.2008.10.067.

[9] K.-C. Lee, B.E. Rittmann, Applying a novel autohydrogenotrophic hollow-fiber membrane biofilm reactor for denitrification of drinking water, Water Res. 36 (2002) 2040–2052. <http://www.ncbi.nlm.nih.gov/pubmed/12092579>.

[10] S.J. Ergas, A.F. Reuss, Hydrogenotrophic denitrification of drinking water using a hollow fibre membrane bioreactor, J. Water Supply Res. Technol. 50 (3) (2001) 161–171.

[11] J.H. Hwang, N. Cicek, J.A. Oleszkiewicz, Achieving biofilm control in a membrane biofilm reactor removing total nitrogen, Water Res. 44 (2010) 2283–2291, http://dx.doi.org/10.1016/j.watres.2009.12.022.

[12] H.P. Zhao, A.O. Valencia, Y. Tang, B.O. Kim, S. Vanginkel, D. Friese, et al., Removal of multiple electron acceptors by pilot-scale, two-stage membrane biofilm reactors, Water Res. 54 (2014) 115–122.

[13] K.-C. Lee, B.E. Rittmann, Effects of pH and precipitation on autohydrogenotrophic denitrification using the hollow-fiber membrane-biofilm reactor, Water Res. 37 (2003) 1551–1556, http://dx.doi.org/10.1016/S0043-1354(02)00519-5.

[14] Z. Feleke, Y. Sakakibara, A bio-electrochemical reactor coupled with adsorber for the removal of nitrate and inhibitory pesticide, Water Res. 36 (2002) 3092–3102, http://dx.doi.org/10.1016/S0043-1354(01)00538-3.

[15] M. Zhou, W. Fu, H. Gu, L. Lei, Nitrate removal from groundwater by a novel three-dimensional electrode biofilm reactor, Electrochim. Acta 52 (2007) 6052–6059, http://dx.doi.org/10.1016/j.electacta.2007.03.064.

[16] S. Mousavi, S. Ibrahim, M.K. Aroua, S. Ghafari, Development of nitrate elimination by autohydrogenotrophic bacteria in bio-electrochemical reactors – a review, Biochem. Eng. J. 67 (2012) 251–264.

[17] S. Szekeres, I. Kiss, T.T. Bejerano, M.I.M. Soares, Hydrogen-dependent denitrification in a two-reactor bio-electrochemical system, Water Res. 35 (2001) 715–719, http://dx.doi.org/10.1016/S0043-1354(00)00300-6.

[18] M. Green, S. Tarre, R. Epsztein, High rate hydrogenotrophic reactor for denitrification of groundwater. IL Patent Application No. 240631 filed on 17.08.15.

[19] C. Glass, J. Silverstein, Denitrification kinetics of high nitrate concentration water: pH effect on inhibition and nitrite accumulation, Water Res. 32 (1998) 831–839, http://dx.doi.org/10.1016/S0043-1354(97)00260-1.

[20] B. Rezania, N. Cicek, J.A. Oleszkiewicz, Kinetics of hydrogen-dependent denitrification under varying pH and temperature conditions, Biotechnol. Bioeng. 92 (2005) 900–906, http://dx.doi.org/10.1002/bit.20664.

[21] G.T. Daigger, J.P. Boltz, Trickling filter and trickling filter-suspended growth process design and operation: a state-of-the-art review, Water Environ. Res. 83 (2011) 388–404, http://dx.doi.org/10.2175/106143010X12681059117210.

[22] T. Wik, Trickling filters and biofilm reactor modelling, Rev. Environ. Sci. Biotechnol. 2 (2003) 193–212.

[23] M. Prosnansky, Y. Sakakibara, M. Kuroda, High-rate denitrification and SS rejection by biofilm-electrode reactor (BER) combined with microfiltration, Water Res. 36 (2002) 4801–4810, http://dx.doi.org/10.1016/S0043-1354(00)00300-6.

[24] C. Lu, P. Gu, P. He, G. Zhang, C. Song, Characteristics of hydrogenotrophic denitrification in a combined system of gas-permeable membrane and a biofilm reactor, J. Hazard. Mater. 168 (2009) 1581–1589, http://dx.doi.org/10.1016/j.jhazmat.2009.03.051.

[25] R. Grommen, M. Verhaege, W. Verstraete, Removal of nitrate in aquaria by means of electrochemically generated hydrogen gas as electron donor for biological denitrification, Aquac. Eng. 34 (2006) 33–39, http://dx.doi.org/10.1016/j.aquaeng.2005.03.007.

[26] C.C. Chang, S.K. Tseng, H.K. Huang, Hydrogenotrophic denitrification with immobilized *Alcaligenes eutrophus* for drinking water treatment, Bioresour. Technol. 69 (1999) 53–58, http://dx.doi.org/10.1016/S0960-8524(98)00168-0.

[27] B. Rezania, J.A. Oleszkiewicz, N. Cicek, Hydrogen-dependent denitrification of water in an anaerobic submerged membrane bioreactor coupled with a novel hydrogen delivery system, Water Res. 41 (2007) 1074–1080, http://dx.doi.org/10.1016/j.watres.2006.11.016.